




Hyperspectral imaging for small-scale analysis of *Hordeum vulgare* L. leaves under the benzo[a]pyrene effect

Pavel Dmitriev¹ · Boris Kozlovsky¹ · Tatiana Minkina¹ · Vishnu D. Rajput¹  · Tamara Dudnikova¹ ·
Andrey Barbashev¹ · Maria Aleksandrovna Ignatova¹ · Olga Anatolievna Kapralova¹ · Tatiana Viktorovna Varduni¹ ·
Valeriy Konstantinovich Tokhtar¹ · Ekaterina Petrovna Tarik¹ · İzzet Akça² · Svetlana Sushkova¹

Received: 21 October 2021 / Accepted: 12 February 2022 / Published online: 16 February 2022
© The Author(s), under exclusive licence to Springer-Verlag GmbH Germany, part of Springer Nature 2022

Abstract

Hyperspectral imaging is a newly developed approach to estimate the current state of the plants and to develop the methods of soil and plant ecological state improvement under the effect of different sources. The study was devoted to the novel approach of hyperspectral imaging application in the case of persistent organic pollutants (POP) uptake by plants. *Hordeum vulgare* L. was used as a test plant and grown on the soil artificially contaminated by benzo[a]pyrene (BaP) in the doses of 20, 100, 200, 400, and 800 ng g⁻¹, which corresponds to 1, 5, 10, 20, and 40 maximum permissible concentrations (MPC) and correlates with the level of soil pollution near industrial facilities in the Rostov Region (Russian Federation). It was analyzed a group of indexes responsible for plants stress, consists of broadband greenness group, narrowband greenness group, light use efficiency group, and leaf pigments group. Benzo[a]pyrene had a stronger effect on the efficiency of the photosynthesis process than on the content of chlorophylls. In the phase of active adaptation to stress in *H. vulgare*, the content of photosynthetic pigments was increased. The proposed method for selecting spectral profiles by cutting off profiles that do not belong to a plant, based on the NDVI value can be effectively used for the estimation of the plants stress under the BaP contamination and for future perspectives in the most suitable way for the application of the plant's growth stimulants.

Keywords Hyperspectral image · Vegetation index · Benzo[a]pyrene · *Hordeum vulgare* L. · Soil contamination · Uptake

Introduction

Environmental pollution with persistent organic pollutants (POP) and their impact on environmental elements, is of increasing interest due to their large-scale distribution in the ecosystem (Bayen 2012; Shen et al. 2013, Wilson and Jones 1993). Among the POP, polycyclic aromatic hydrocarbons (PAHs) occupied primary position because of their stability in landscape components, high toxicity, potential mutagenic, teratogenic, and carcinogenic effects which strongly affect

human health's and other living organisms (El-Shahawi et al. 2010; Hamid et al. 2018; Liu et al. 2005).

The most dangerous representative of PAHs is benzo[a]pyrene (BaP) characterized by a large lipophilic molecule containing 5 condensed benzene rings. Unlike other widespread pollutants of the PAH group, BaP belongs to carcinogens of the first hazard class (IARC list) indicated by the International Agency for Research on Cancer.

The content of BaP reached 350 ng g⁻¹ near a large energy enterprise in the Rostov Region (Russia), working on the combustion of the low-quality coal (Sushkova et al. 2017a, b). There are data on the BaP content in soils of the Orlando city (USA), where BaP value reached 1500 ng g⁻¹ (Emengini et al. 2013a, b). The average BaP content in Chinese soils was determined at the level 124 ng g⁻¹ (Yu et al. 2019). The world community has not reached a consensus on the regulation of BaP content in soils. In the Russian Federation, the maximum permissible concentration of BaP in soils is 20 ng g⁻¹ (GN-2.1.7.2041–06 2006), and in Canada, it

Responsible Editor: Elena Maestri

✉ Vishnu D. Rajput
rajput.vishnu@gmail.com

¹ Academy of Biology and Biotechnology, Southern Federal University, Rostov-on-Don 344090, Russia

² Faculty of Agriculture, Department of Plant Protection, Ondokuz Mayıs University, Samsun, Turkey

should not exceed 600 ng g^{-1} (CCME (Canadian Council of Ministers of the Environment) 2010). A number of countries use a comprehensive pollutant hazard assessment based on the results of keeping a group of PAHs, where BaP is mentioned in each of these lists. In the Netherlands, the sum of 10 PAHs concentrations, including BaP, should not exceed 1000 ng g^{-1} (VROM 1994) and 300 ng g^{-1} according to Swedish standards (Brezet 2000). However, plant dysfunction begins when they grow in soil contaminated with as little as 20 ng g^{-1} BaP (Fedorenko et al. 2021).

The ubiquitous distribution of BaP in the environment is due to the activities of industrial sectors to a larger extent, enterprises of the fuel and energy complex, vehicles, and oil spills (Yu et al. 2019; Yurdakul et al. 2019). The soil is a sink of biogeochemical cycles of these hazardous chemical elements since there is a redistribution of all substances coming from the parent rocks, with vegetation loss and deposition from the atmosphere; therefore, soil pollution is reflected in the entire ecosystem as a whole (Rajput et al. 2018; Sushkova et al. 2019b)). Mostly, industrial and agricultural lands are located in close proximity to each other. As a result, soils used for agriculture accumulate PAHs, including BaP (Boente et al. 2020; Jia et al. 2017; Li et al. 2017; Sushkova et al. 2020).

Toxicity caused by BaP significantly reduced the plant growth and development in various crop plants. The decreased rate of seed germination, root growth, and aerial plant parts have been reported after BaP exposure (Sivaram et al. 2018; Sun et al. 2011; Sushkova et al. 2021a, b). Regardless of the noticeable changes in the morphometric characteristics of plants, the BaP concentration at the level even 20 ng g^{-1} in the soil showed changes at the ultrastructural level of cellular-subcellular organization. At a concentration of $200\text{--}400 \text{ ng g}^{-1}$ BaP in the soil, multiple changes were noted in the vacuole, cytoplasm, nucleus, and mitochondria (Fedorenko et al. 2021). The disorganization of the nucleus, mitochondria, and chloroplasts were also observed in the mangrove plant tissues grown on fuel oil or oil polluted medium (Naidoo 2016; Naidoo and Naidoo 2017). It was shown that the changes in structure and ultrastructural levels in roots and leaves tissues directly affects the metabolic and physiological processes of plants (Fedorenko et al. 2021).

The use of spectral imaging has proven its effectiveness in recording changes in the physio-biochemical parameters of plants caused by soil contamination with hydrocarbons (Arellano et al. 2015; Emengini et al. 2013a, b; Lassalle et al. 2018; Sanches et al. 2013; Shit et al. 2021). Changes in biophysical and biochemical parameters of leaves lead to changes in reflectivity that help to distinguish the healthy from diseased vegetation (Das et al. 2021; Lassalle et al. 2018; Rosso et al. 2005). The effect of PAHs, including BaP, on the photosynthetic apparatus of plants is expressed in a

decrease in the total content of chlorophyll (Sivaram et al. 2018). Under the influence of PAHs and petroleum hydrocarbons, a decrease in transpiration rate, chlorophyll a and b contents, and carotenoids were found (Lassalle et al. 2019; Zhu et al. 2014). At the same time, the ratio of chlorophyll A to chlorophyll B increases, which indicates plant stress caused by the absorption of BaP (Sivaram et al. 2018). The reflectivity of leaves varies depending on the species resistance of plants to PAHs and the growing season. The reflectivity of the leaves differs depending on the growing season and the species of the studied plant (Lassalle et al. 2019). When soil is treated with phenanthrene, a decrease in the reflectivity of various species plants is observed, which is closely related to a decrease in the amount of chlorophyll. The spectral parameters (red edge slope and area) responded to the phenanthrene, consistently with the plant parameters (Zhu et al. 2014; Lassalle et al. 2019), absorption of chlorophyll and carotenoids (Emengini et al. 2013a, b; Zhang et al. 2017; Lassalle et al. 2019). At the present stage, hyperspectral methods make it possible to assess the degree of plant disease and crop loss if it is used for an agricultural area (Bock et al. 2010; Khan et al. 2018; Benelli et al. 2020). The identification of changes in the spectral characteristics of plants in response to stress during soil pollution occurs before the moment of visible disturbances in plant life, and allows early detection of environmental pollution (Das et al. 2021; Emengini et al. 2013a, b), which is important in the conditions of agricultural crops production. At the same time, these methods of analysis potentially simplify the assessment of environmental risks associated with the contamination of vast areas with various pollutants. This significantly reduces the time to take measures to eliminate undesirable effects for plants as objects of agricultural production, as well as to preserve their species diversity and the ecosystem as a whole.

Thus, the spectral imaging is a perceptive express method for assessing the stress of plants growing on PAH-contaminated soil. Since plants react differently to soil pollution, study of the species responsive to physiological and biochemical levels for different crops become an important component in the development of monitoring and control systems for sustainable agricultural products.

Material and methods

Experimental set-up

The soils sampled from the top layer of 0–20 cm in the virgin area of the Persianovskiy soil nature reserve (Russia, Rostov region) were used in present experiment. The collected soils are classified as Haplic Chernozem with the following characteristics: content of physical clay 52%, silt 30%, humus

4.2%, pH_{water} 7.5, CaCO₃ 0.4%, and EC 33 cmol (+)/kg. The soil was sieved through a sieve with a diameter of 1 mm and placed 2 kg pots in 4-kg size plastic pots. A solution of BaP in acetonitrile was added to the soil surface based on the creation of a pollutant concentration in the soil of 20, 100, 200, 400, and 800 ng g⁻¹, which corresponds to 1, 5, 10, 20, and 40 MPC. The doses of BaP introduction into the soil of the model experiment correspond to the content of the pollutant in the industrial regions of the Rostov Region (Sushkova et al. 2019a, 2019b). The original and polluted soils with pure acetonitrile were used as controls. The experiment was performed in triplicate for each experience.

Conditions for the vegetation experiment

The soils spiked with pollution in the pots were incubated under the climatic conditions close to natural for 3 months, pouring distilled water over it as needed to maintain optimal moisture content to preventing it from drying out. *H. vulgare* was used as a test culture crop, which is one of the main agricultural crops in the Rostov region of Russian Federation (Mandzhieva et al. 2020). The 30 health seeds of *H. vulgare* were sown in each pots spiked with pollutions.

Extraction of BaP

Extraction of BaP from soils and plants was carried out with hexane in triplicate. To establish the completeness of the extraction of BaP from the soil, a blank experiment was carried out with the introduction of solutions with a given concentration into the soil (addition method). In this case, the additive was introduced with an acetonitrile solution of the pollutant into a sample of soil weighing 1 g. The additives were introduced at concentrations of 10, 25, and 50 ng g⁻¹. BaP was extracted from the soils and plants by the standard method using for the removal of the interfering lipid components by saponification method using boiling of sample in 2% KOH solution in ethanol with next extraction with n-hexane (Sushkova et al. 2017a, b, 2021a). The completeness of BaP extraction was determined by the matrix spike method. After the samples were analyzed by HPLC method according to the certified procedures (MUK 4.1.1274–03.4.1, 2003; ISO-13877–2005 2005) using the system with fluorometric detection 1260 Infinity Agilent (USA). All research results were performed in threefold analytical replication. The BaP peak in the chromatogram of the soil extract was identified by comparing the BaP retention time in the analysis of the extract and the standard sample with simultaneous detection on two detectors. This makes it possible to identify the BaP peak with a sufficiently high degree of reliability and to more accurately determine its concentration in the extract. To assess the level of BaP accumulation by vegetation growing on monitoring sites, the ratios of the

BaP content in the roots to its content in the soil, as well as BaP in the stems to its content in the roots, were calculated. These ratios characterize the intensity of biochemical absorption and the effect of retention of the studied carcinogen by various plant organs, which characterizes the resistance of plants to pollution.

Canopy reflectance: spectral imaging

Surveys to obtain a hyperspectrum were carried out on days 14 and 28 after the emergence of *H. vulgare* seedlings, at the stage of seedling growth and tillering. Hyperspectral images were taken using a Cubert UHD-185 hyperspectral camera (Aasen et al. 2015; Bareth et al. 2015). The shooting was carried out in the period from 12 to 13 o'clock in sunlight in cloudless weather. For the survey, the plants were not removed from the pots because of the danger of modifying their physiological and biochemical characteristics. The camera lens was located at a height of 50 cm from the plant object and was at right angles to the surface of the pots. Each pot was recorded three times. One image is presented in the form of one panchromatic image, size 1000 × 1000 pixels and 125 hyperspectral images, size 50 × 50 pixels. The spatial resolution of the obtained hyperspectral data was approximately 30 mm². The reflected electromagnetic radiation from the leaves was recorded in the range of 450–950 nm.

The leaf surfaces of the plants had different degrees of illumination and at various orientation angles relative to the camera lens. In order to cut off pixels from the sample that capture the substrate and the pots or simultaneously capture the substrate and the plant surface, the NDVI (normalized difference vegetation index) threshold was set to 0.2. That is only those spectral profiles which NDVI values were more than 0.2, and were selected into the sample for further statistical processing. A hyperspectral image of growing pots (control variant) is shown in Fig. 1.

In the present work, following groups indices were calculated.

Broadband greenness group. These indices were determined from the data in the wide spectral zones. This groups importance is associated with chlorophyll content, leaf area, density, and structure of vegetation. Simple ratio index (SR) and NDVI were calculated from this group's indices.

Narrowband greenness group. This groups index was calculated from the data in narrow spectral zones. In contrast to previous groups indices, these groups indices were more sensitive and respond to even small changes in chlorophyll content, leaf area, density, and structure of vegetation. From this group of indices, the modified red edge simple ratio index (mSR705),

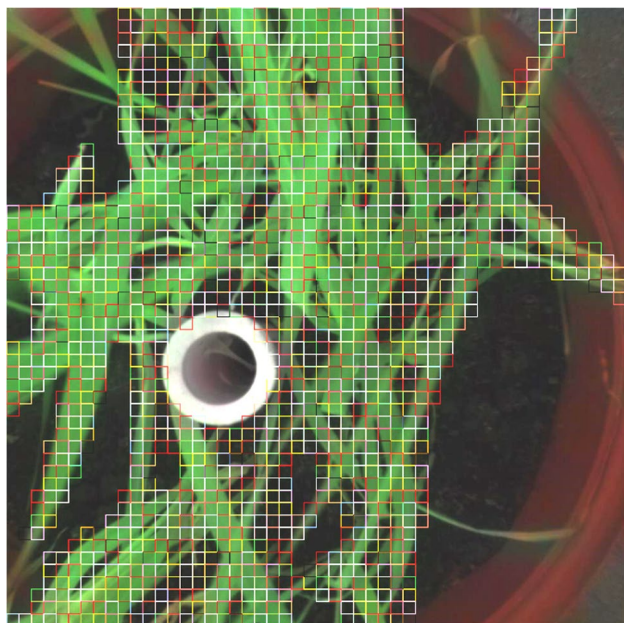


Fig. 1 Recording of hyperspectral image of a *H. vulgare* plants (control variant)

normalized difference vegetation index 2 (NDVI705 or NDVI2), Vogelmann index 1 (Vogelman1), red edge position index_linear interpolation (REP_LI) were calculated.

Light use efficiency group. The indices of this group reflect the efficiency of the photosynthesis process. It correlates with the absorption of photosynthetically active radiation, the efficiency of carbon assimilation, and growth activity. From this group of indices, the photochemical reflectance index (PRI) was calculated.

Leaf pigments group. The indices reflect the content of carotenoids and anthocyanins. Changes in these contents indicate stress in plants. These indices do not include chlorophyll. From this group of indices, carotenoid reflectance index 1 and carotenoid reflectance index 2 (CRI1 and CRI 2) were calculated.

Statistical processing of results

Regression analysis was performed using the Sigmaplot 12.5 software. Mathematical processing of the hyperspectral survey results was carried out in the environment for statistical calculations R (R Core Team), using the hsdar package (Lehnert et al. 2018). To check the normal distribution of vegetation indices, the following test methods were used: Shapiro–Wilk, Pearson’s chi-squared, Lilliefors, Cramér–von Mises. Comparison of the values of vegetation indices in different variants was carried out using the Wilcox test for independent samples (Mann–Whitney *U*-test).

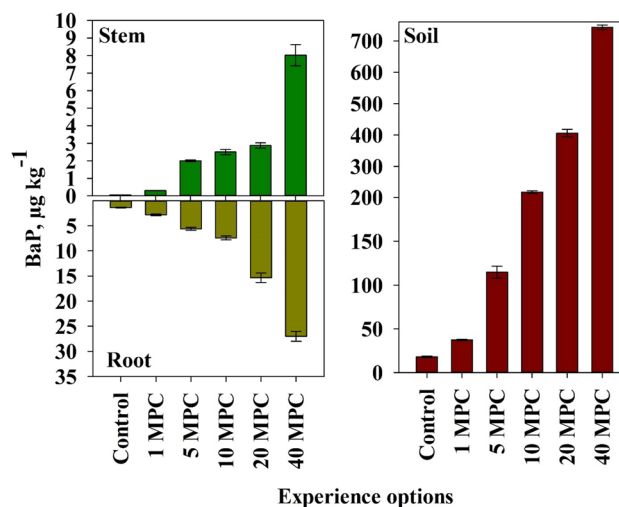


Fig. 2 The content of BaP in the soil and their accumulation in the roots and stems of *H. vulgare* under the conditions of a model experiment. Note: The error bars on the chart represent the standard deviation

Results and discussion

From the present study, it was found that the content of BaP in the soil of the control sample does not exceed the MPC and corresponds to 18 ng/g. The introduction of the pollutant promoted the accumulation of BaP in the soil. As the dose of the introduced pollutants increased, the content of BaP also in the soil increased by 2, 6, 12, 23, and 41 folds with the introduction of 1, 5, 10, 20, and 40 MPC pollutants, respectively (Fig. 2).

H. vulgare grown on soil without the BaP application showed the pollutant accumulation in the roots—1 ng g⁻¹, and in the stems—less than 0.1 ng g⁻¹. The accumulation of BaP in the root of *H. vulgare* was higher than in the stem. The increase in the content of BaP in various parts of plants is proportional to the dose of BaP applied into the soil. The content of BaP increased by 3, 6, 7, 15, and 27 folds under the condition of the initial introduction of pollutants into the soil at a dose of 1, 5, 10, 20, and 40 MPC, respectively. The stem part of *H. vulgare* was more sensitive to changes in the content of BaP in the soil and root part, since the accumulation of BaP in the stems increases to a greater extent. With the initial application of BaP to the soil at a dose of 1, 5, 10, 20, and 40 MPC, the accumulation of the pollutant in the stem part increases by 6, 40, 50, 57, and 160 folds higher relative to the control plants, respectively (Fig. 2).

The BaP has a low migratory activity in soil. The ratio of the BaP content in the root to its content in the soil was 1:0.055. This ratio between stem and root is less and was 1:0.050, these changes indicate a decrease in the migration activity of the pollutant on the root-stem system. With the introduction of the pollutant into the soil at a dose of 1

MPC, the ratio of BaP in the root to its content in the soil increased 1.5-folds. A further increase in the dose of the pollutant applying into the soil from 1 to 40 MPC leads to a decrease in this indicator.

The ratio of the BaP content in the stems to its content in the roots increases with an increase in the dose of BaP application. This pattern was observed at the initial addition of a pollutant into the soil with a dose of no more than 10 MPC. At the same time, no more than 7 ng g⁻¹ of BaP was accumulated in the root tissues. An increase in the dose of BaP application into the soil upto 20 MPC leads to a decrease in the ratio of the pollutant content in the stems to its content in the roots. This fact indicates the activation of barrier mechanisms in the stem part of plants in relation to the migration activity of the pollutant at a BaP content in the root of 7 ng g⁻¹. A subsequent increase in the dose of BaP application to the soil upto 40 MPC leads to a repeated increase in the stems/ roots ratio, which indicates the suppression of the barrier function of *H. vulgare* (Fig. 3).

The relationship was revealed between the accumulation of BaP in the root and the content of pollutants in the soil, as well as the accumulation of BaP in the stem and the content of pollutants in the roots (Fig. 4).

It was found that the absorption of BaP by the roots occurs nonlinearly and is described by the Eq. (1):

$$y = a \times x^b \tag{1}$$

where y is the BaP content in the root part of *H. vulgare*, x is the BaP content in the soil, a is the scaling factor, and b is the rate of growth of the function.

As a result of approximating the results of the BaP content in the root part of the plant versus the pollutant content in the soil at p -level < 0.0001, the following equation was obtained:

$$y = 0.063 \times x^{0.917} \tag{2}$$

The nonlinearity of BaP migration increases from root to stem. This indicates the presence of a biological barrier at the border of the root-stem transition. The relationship between the accumulation of BaP by the stem part of the plant and the content of the pollutant is fundamentally described by a logarithmic equation with two parameters:

$$f = \text{if}(x - x_0 > 0; a \times \ln(|x - x_0|); 0)$$

where x is the BaP content in the root part of *H. vulgare*, y is the BaP content in the stem part of *H. vulgare*, a is the scaling factor, \ln is the natural logarithm, x_0 is the absolute minimum.

$$f = \text{if}(x - 0,618 > 0; 1,693 \times \ln(|x - 0,618|); 0)$$

In the course of the research, it was found that the histogram of the distribution of spectral profiles obtained

Fig. 3 The ratio of the BaP content in the root to its content in the soil, as well as the ratio of the BaP content in the stem to its content in the roots. Note: The error bars on the chart represent the standard deviation

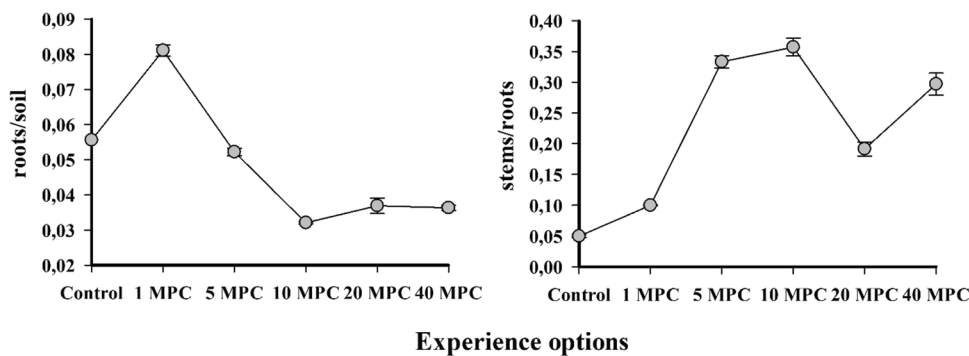
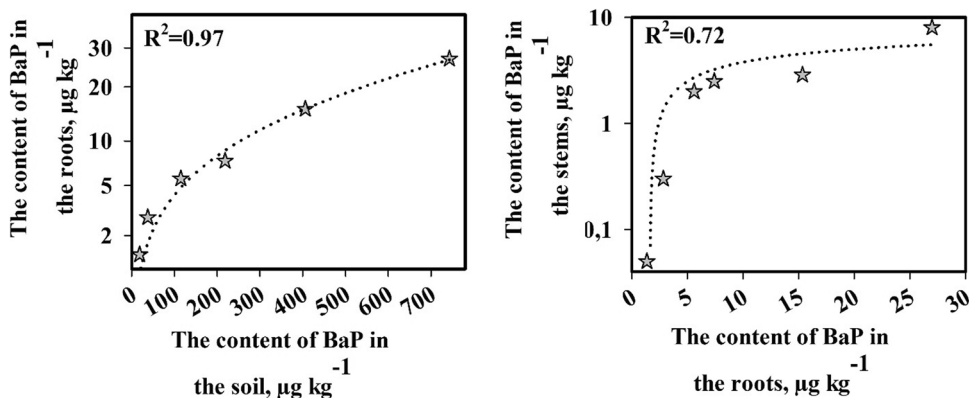


Fig. 4 Accumulation of BaP in the root, depending on the pollutant content in the soil, as well as the accumulation of BaP in the stem, depending on the pollutant content in the roots



from the entire surface of the growing vessel has two peaks according to the value of the NDVI index (Fig. 5).

The first peak lies in the region of NDVI values equal to 0.2, the second peak in the region of NDVI value equal to 0.7. This is due to the fact that the camera recorded both reflection from plants and from the substrate and parts of the growing plants in the pots. Therefore, when processing hyperspectral images, it was tried to cut off pixels that do not belong to plants and mixed pixels. Mixed pixels—pixels that capture a plant and a medium or a plant and a vessel.

The choice of “clean” pixels directly by the operator has a large subjective error. The difference in the results of statistical processing of samples formed by different operators reaches 10%. Therefore, a unified mechanistic approach was used for all images—spectral profiles were used to calculate VI, giving NDVI in the range from 0.2 to 1.0.

The lower bound for the NDVI value was chosen based on the existing experience in constructing regression models linking to the NDVI value and crop yield (Durgun et al. 2020; Vannoppen et al. 2020). All other vegetation indices were calculated based on the spectral profiles selected in this way. After such manipulations, the vegetation indices from the Greenness groups reflect to a greater extent the content of chlorophylls and a lesser extent leaf surface area, density, and structure of vegetation. The nature of the distribution of vegetation indices in magnitude was studied. The distribution of vegetation indices SR, NDVI2, Vogelmann, PRI, calculated before and after “cleaning” hyperspectral images, are shown in magnitude in Fig. 6.

It has been established that in the overwhelming majority of cases the indices were distributed by value, not according to the normal law. Therefore, the comparison of the values of the indices of the control and experimental variants was carried out using the nonparametric Wilcoxon test for independent samples (Mann–Whitney U -test).

During the first observation period, the values of the broadband greenness indices (SR, NDVI) and narrowband

greenness indices (mSR, NDVI2, Vogelmann1) under the influence of various doses of BaP provided a characteristic response curve for the value of the acting factor. With an increase in the dose of the pollutant introduced into the soil, a gradual increase in the indices associated with the content of chlorophylls was observed. At a dose of 20 MPC, these values reach a maximum; however, at a dose of 40 MPC, it begins to decrease. The inhibitory effect of BaP in the first period was not recorded, since even with its introduction into the soil at a dose of 40 MPC, the value of the vegetation indices from the greenness group was higher than in the control. Interestingly, the REP_Li index deviates less from control by variants than other indexes.

BaP had a stronger effect on the efficiency of the photosynthesis process than on the content of chlorophylls. This is evidenced by the more intensive change in the index of the efficiency of the photosynthesis process PRI in comparison with the indices from the greenness groups. The indices of the leaf pigments group—CRI1, CRI 2, the values of which correlate with the content of carotenoids and anthocyanins, vary by variants randomly. An increase in the content of these pigments may indirectly indicate the presence of stress. In general, this value is higher for plants growing under conditions with the introduction of BaP into the soil as compared to *H. vulgare* in the control variant (Fig. 7).

Repetition of the experiment on the second observation (date of sowing 28 days) showed the same results as in the first shooting date. The general nature of the change in the values of vegetation indices with an increase in the concentration of BaP in the substrate did not change. However, after an increase in the values of the vegetation indices greenness in variants with BaP concentrations of 1, 5, and 10 MPC, their values begin to reduce already at a concentration of 20 MPC. In variant 40 MPC, an inhibitory effect was recorded—the value of SR, mSR2 NDVI NDVI2 Vogelmann was significantly lower than the control one.

The observed change in the physiological characteristics of plants can be explained based on the Selye triad (Selye 1990), which describes the nature of the body’s response to stress. At the time of the first measurement of the spectral reflection, *H. vulgare* plants had already passed the phase of the primary inductive stress response and were in the second phase, the adaptation phase (in this case, active adaptation occurs). In the phase of active adaptation, along with other biochemical processes, there is an increase in the activity of the functioning of mitochondria and chloroplasts and, accordingly, the level of energy supply.

On the other hand, an increase in the level of energy supply of a plant organism can be achieved not only by increasing the activity of chloroplast functioning (increasing the efficiency of photosynthesis), but also by increasing the concentration of chlorophylls. This is indicated by an increase in the content of chlorophylls in the experimental plants.

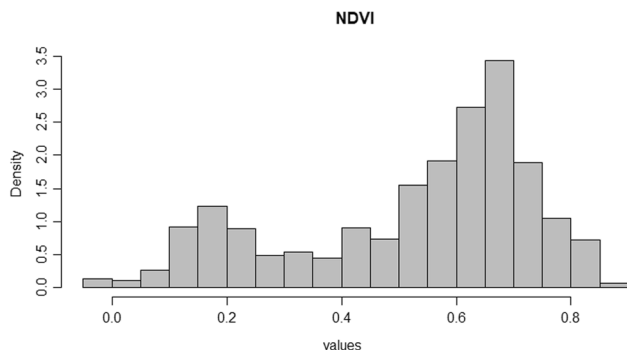
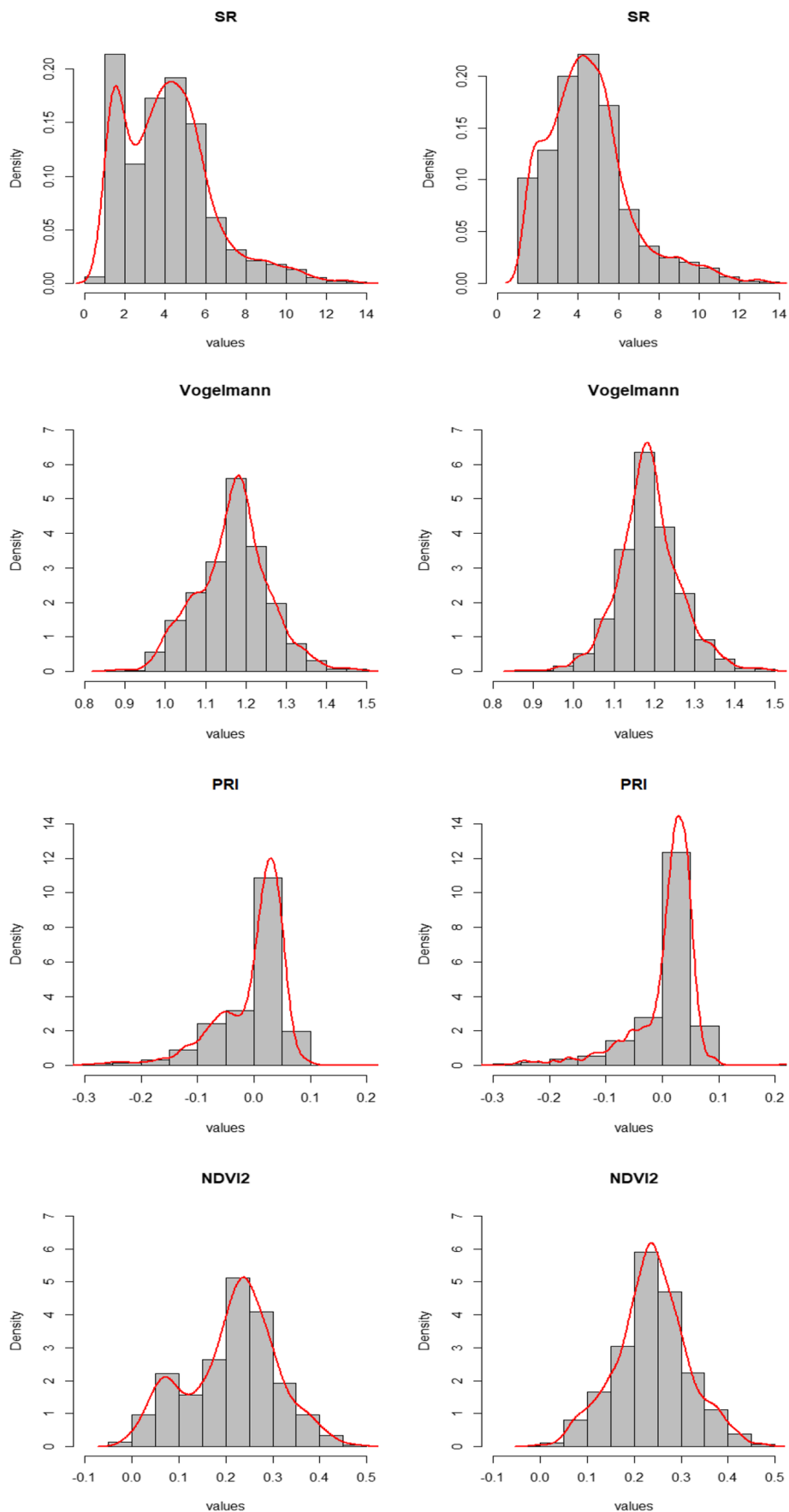


Fig. 5 Histogram of the distribution of the spectral profiles of the surface of the growing plants according to the NDVI value. Test case, the first shooting date

Fig. 6 Distribution of VI by size before “cleaning”—on the left and after “cleaning”—on the right of hyperspectral images



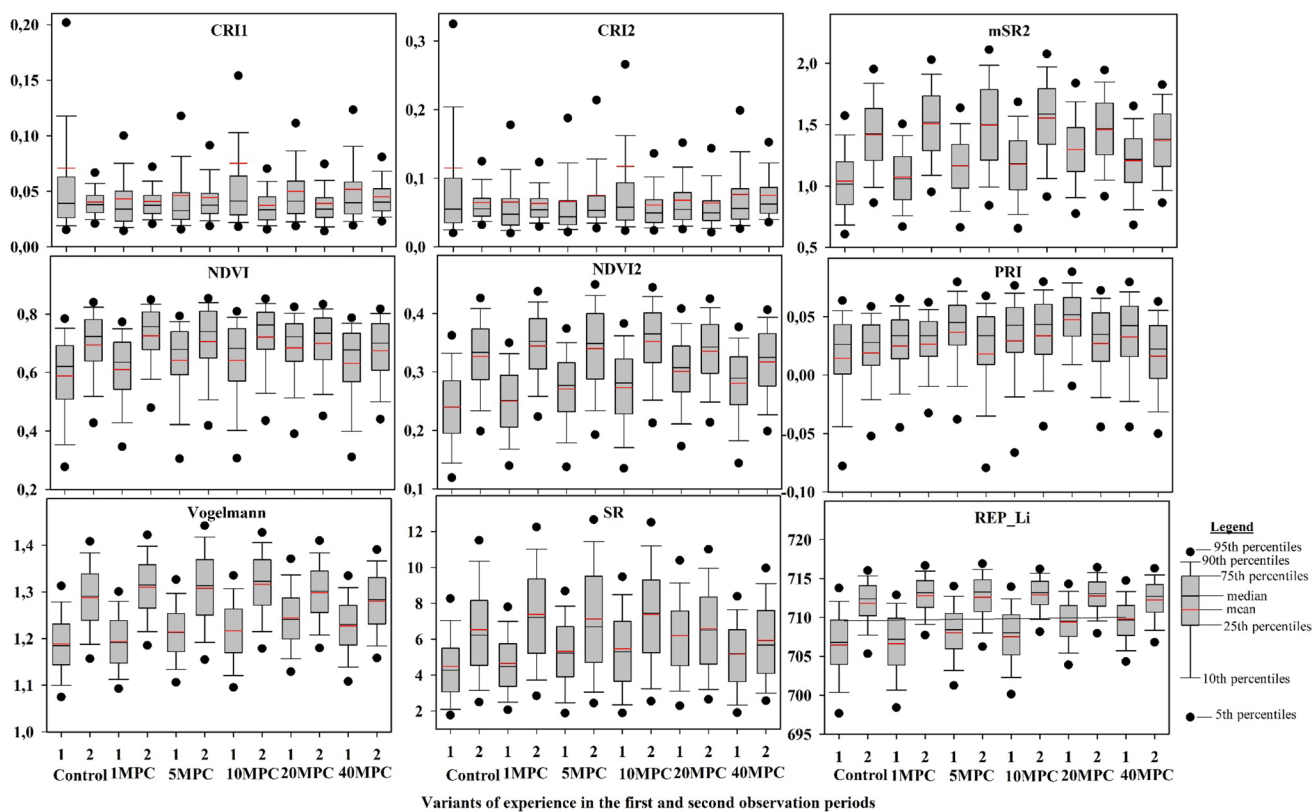


Fig. 7 Values of vegetation indices on the first and second dates of measurements of *H. vulgare*, depending on the dose of application of BaP to the soil

We assume that the second hyperspectral survey recorded the third phase of *H. vulgare* response to stress—the phase of exhaustion.

At this stage, in conditions of an increase in the strength of the effect and a gradual exhaustion of the protective capabilities of the plant's organism, nonspecific reactions dominate. The depletion phase, in particular, is characterized by a violation of the ultrastructure of chloroplasts, which can lead to a decrease in the content of chlorophylls in the cell. This is indirectly confirmed by the decrease in the vegetation indices greenness at the maximum concentrations of BaP in comparison with the control.

Conclusion

It was found that BaP contamination of the soil led to toxicant accumulation in the *H. vulgare* plants. The ratio of the BaP content in the stems to its content in the roots, as well as steam, increased linearly to the increasing of the applied BaP dose from 1 to 40 MPC of BaP. Based on the Selye triad, it was shown that the phase of *H. vulgare* adaptation to stress is characterized by an increase in the vegetation indices SR, NDVI, mSR, NDVI2, Vogelmann1. At the

same time, in the depletion phase of *H. vulgare*, there is a significant decrease in the values of SR, mSR2 NDVI NDVI2 Vogelmann. In the phase of active adaptation to stress in *H. vulgare*, the content of photosynthetic pigments was increased. The proposed method for selecting spectral profiles by cutting off profiles that do not belong to a plant, based on the NDVI value, it can be effective in similar to case that described in the work. For example, in hyperspectral photography of crops, tree crowns, when leaves are captured at different angles and with different degrees of illumination, as well as elements of the trunk, branches and objects that do not belong to the plant.

Author contribution All authors contributed to the study conception and design. P.D., B.K. T.D., and A.B. collected the data, performed the analysis, and S.S., P.D. A.B., and V.D.R. drafted the manuscript. T.M., T.V.V., and S.S. supervised the work and contributed to the interpretation of the results. V.D.R., M.A.I., O.A.K. V.K.T., E.P.T., and I.A. provided critical feedback and helped shape the analysis and manuscript. All authors read and approved the final manuscript.

Funding The research was financially supported by the Ministry of Science and Higher Education of the Russian Federation within the framework of the state task in the field of scientific activity (no. 0852–2020-0029), RFBR no. 19–29-05265_mk.

Declarations

Competing interests The authors declare no competing interests.

References

- Aasen H, Burkart A, Bolten A, Bareth G (2015) Generating 3D hyperspectral information with lightweight UAV snapshot cameras for vegetation monitoring: from camera calibration to quality assurance. *ISPRS J Photogramm Remote Sens* 108:245–259
- Arellano P, Tansey K, Balzter H, Boyd DS (2015) Detecting the effects of hydrocarbon pollution in the Amazon forest using hyperspectral satellite images. *Environ Pollut* 205:225–239
- Bareth G, Aasen H, Bendig J, Gnyp ML, Bolten A, Jung A, Michels R, Soukkamäki J (2015) 7 low-weight and UAV-based hyperspectral full-frame cameras for monitoring crops: spectral comparison with portable spectroradiometer measurements. Unmanned aerial vehicles (UAVs) for multi-temporal crop surface modelling, 103
- Bayen S (2012) Occurrence, bioavailability and toxic effects of trace metals and organic contaminants in mangrove ecosystems: a review. *Environ Int* 48:84–101
- Benelli A, Cevoli C, Fabbri A (2020) In-field hyperspectral imaging: an overview on the ground-based applications in agriculture. *J Agric Eng* 51(3):129–139
- Bock CH, Poole GH, Parker PE, Gottwald TR (2010) Plant disease severity estimated visually, by digital photography and image analysis, and by hyperspectral imaging. *Crit Rev Plant Sci* 29(2):59–107
- Boente C, Baragaño D, Gallego J (2020) Benzo [a] pyrene sourcing and abundance in a coal region in transition reveals historical pollution, rendering soil screening levels impractical. *Environ Poll* 266:115341
- Brezet, H. (2000), Product-Service Substitution: Examples and Cases from the Netherlands, ‘Funktionsförsäljning’ – product-service systems, Stockholm, Swedish EPA, AFR-report 299.
- CCME (Canadian Council of Ministers of the Environment) (2010) Canadian soil quality guidelines for the protection of environmental and human health: carcinogenic and other PAHs. In: Canadian environmental quality guidelines, 1999, 200 Winnipeg, Canada. https://www.esdat.net/environmental%20standards/canada/soil/rev_soil_summary_tbl_7.0_e.pdf
- Das S, Bhunia GS, Bera B, Shit PK (2021): Evaluation of wetland ecosystem health using geospatial technology: evidence from the lower Gangetic flood plain in India. *Environ Sci Pollut Res*
- Durgun YÖ, Gobin A, Duveiller G, Tychon B (2020) A study on trade-offs between spatial resolution and temporal sampling density for wheat yield estimation using both thermal and calendar time. *Int J Appl Earth Obs Geoinf* 86:101988
- El-Shahawi M, Hamza A, Bashammakh A, Al-Saggaf W (2010) An overview on the accumulation, distribution, transformations, toxicity and analytical methods for the monitoring of persistent organic pollutants. *Talanta* 80:1587–1597
- Emengini EJ, Blackburn GA, Theobald JC (2013) Discrimination of plant stress caused by oil pollution and waterlogging using hyperspectral and thermal remote sensing. *J Appl Remote Sens* 7:073476
- Emengini EJ, Ezeh FC, Chigbu N (2013b) Comparative analysis of spectral responses of varied plant species to oil stress. *Int J Sci Eng Res* 4(6):1421–1427
- Fedorenko AG, Chernikova N, Minkina T, Sushkova S, Dudnikova T, Antonenko E, Fedorenko G, Bauer T, Mandzhieva S, Barbashev A (2021) Effects of benzo [a] pyrene toxicity on morphology and ultrastructure of *Hordeum sativum*. *Environ Geochem Health* 43:1551–1562
- GN-2.1.7.2041–06 (2006) On the introduction of hygienic standards. - Introduction. 2006–23–01. - M.: Federal Center for Hygiene and Epidemiology of Rosпотrebnadzor
- Hamid N, Syed JH, Junaid M, Mahmood A, Li J, Zhang G, Malik RN (2018) Elucidating the urban levels, sources and health risks of polycyclic aromatic hydrocarbons (PAHs) in Pakistan: implications for changing energy demand. *Sci Total Environ* 619:165–175
- ISO-13877–2005 (2005) Soil quality - determination of polynuclear aromatic hydrocarbons - method using high-performance liquid chromatography
- Jia J, Bi C, Guo X, Wang X, Zhou X, Chen Z (2017) Characteristics, identification, and potential risk of polycyclic aromatic hydrocarbons in road dusts and agricultural soils from industrial sites in Shanghai, China. *Environ Sci Pollut Res* 24:605–615
- Khan MJ, Khan HS, Yousaf A, Khurshid K, Abbas A (2018) Modern trends in hyperspectral image analysis: a review. *Ieee Access* 6:14118–14129
- Lassalle G, Credoz A, Hédacq R, Fabre S, Dubucq D, Elger A (2018) Assessing soil contamination due to oil and gas production using vegetation hyperspectral reflectance. *Environ Sci Technol* 52:1756–1764
- Lassalle G, Fabre S, Credoz A, Hédacq R, Bertoni G, Dubucq D, Elger A (2019) Application of PROSPECT for estimating total petroleum hydrocarbons in contaminated soils from leaf optical properties. *J Hazard Mater* 377:409–417
- Lehnert LW, Meyer H, Obermeier WA, Silva B, Regeling B, Bendix J (2018) Hyperspectral data analysis in R: the hsdar package. arXiv preprint arXiv:1805.05090
- Li Y, Long L, Ge J, Yang L-x, Cheng J-j, Sun L-x, Lu C, Yu X-y (2017) Presence, distribution and risk assessment of polycyclic aromatic hydrocarbons in rice-wheat continuous cropping soils close to five industrial parks of Suzhou, China. *Chemosphere* 184:753–761
- Liu X, Zhang G, Jones KC, Li X, Peng X, Qi S (2005) Compositional fractionation of polycyclic aromatic hydrocarbons (PAHs) in mosses (*Hypnum plumaeformae* WILS.) from the northern slope of Nanling Mountains, South China. *Atmos Environ* 39:5490–5499
- Mandzhieva S, Barakhov A, Minkina T, Chaplygin V, Sushkova S (2020) Assessment of the combined effect of heavy metals and polyaromatic hydrocarbons on the cultural plants. *E3S Web Conf* 175:07006
- MUK 4.1.1274–03. 4.1. Control methods. Chemical factors. Measurement of the mass fraction of benzo(a)pyrene in samples of soils, grounds, bottom sediments and solid waste by HPLC using a fluorometric detector. Methodological guidelines (approved by the Ministry of Health of Russia on 01.04.2003) // Measurement of the mass concentration of chemicals by luminescent methods in environmental objects: collection of guidelines. - M.: Federal Center for State Sanitary and Epidemiological Supervision of the Ministry of Health of Russia, 244–267 p. (2003). (In Russia)
- Naidoo G (2016) Mangrove propagule size and oil contamination effects: does size matter? *Mar Pollut Bull* 110:362–370
- Naidoo G, Naidoo K (2017) Ultrastructural effects of polycyclic aromatic hydrocarbons in the mangroves *Avicennia marina* and *Rhizophora mucronata*. *Flora* 235:1–9
- Rajput VD, Minkina TM, Behal A, Sushkova SN, Mandzhieva S, Singh R, Gorovtsov A, Tsitsuashvili VS, Purvis WO, Ghazaryan KA, Movsesyan HS (2018) Effects of zinc-oxide nanoparticles on soil, plants, animals and soil organisms: a review. *Environ Nanotechnol Monit Manag* 9:76–84
- Rosso PH, Pushnik JC, Lay M, Ustin SL (2005) Reflectance properties and physiological responses of *Salicornia virginica* to heavy metal and petroleum contamination. *Environ Pollut* 137:241–252

- Sanches I, Souza Filho C, Magalhães L, Quitério G, Alves M, Oliveira W (2013) Assessing the impact of hydrocarbon leakages on vegetation using reflectance spectroscopy. *ISPRS J Photogramm Remote Sens* 78:85–101
- Selye G (1990) At the level of the whole organism. Nauka, Moscow, p 212
- Shen H, Huang Y, Wang R, Zhu D, Li W, Shen G, Wang B, Zhang Y, Chen Y, Lu Y (2013) Global atmospheric emissions of polycyclic aromatic hydrocarbons from 1960 to 2008 and future predictions. *Environ Sci Technol* 47:6415–6424
- Shit P, Bhunia G, Das P, Narsimha A (2021) Geospatial technology for environmental hazards
- Sivaram AK, Logeshwaran P, Lockington R, Naidu R, Megharaj M (2018) Impact of plant photosystems in the remediation of benzo [a] pyrene and pyrene spiked soils. *Chemosphere* 193:625–634
- Sun Y, Zhou Q, Xu Y, Wang L, Liang X (2011) Phytoremediation for co-contaminated soils of benzo [a] pyrene (B [a] P) and heavy metals using ornamental plant *Tagetes patula*. *J Hazard Mater* 186:2075–2082
- Sushkova S, Batukaev A, Minkina T, Antonenko E, Dudnikova T, Bauer T, Fedorenko A, Rajput V, Barbashev A, Dorohova N (2019a) Novochoerkassk Power Station emissions effect on PAHs accumulation in the adjoining soils, *Geophysical Research Abstracts*
- Sushkova S, Minkina T, Deryabkina I, Rajput V, Antonenko E, Nazarenko O, Yadav BK, Hakki E, Mohan D (2019b) Environmental pollution of soil with PAHs in energy producing plants zone. *Sci Total Environ* 655:232–241
- Sushkova S, Minkina T, Batukaev A, Dudnikova T, Shavanov M, Adymkhanov L, Barakhov A (2020) Diagnostic ratios of individual polycyclic aromatic hydrocarbons for their identification in soils of power station, *IOP Conference Series: Materials Science and Engineering*. IOP Publishing, 012065
- Sushkova S, Minkina T, Tarigholizadeh S, Rajput V, Fedorenko A, Antonenko E, Dudnikova T, Chernikova N, Yadav BK, Batukaev A (2021a) Soil PAHs contamination effect on the cellular and sub-cellular organelle changes of *Phragmites australis* Cav. *Environ Geochem Health* 43:2407–2421
- Sushkova S, Minkina T, Turina I, Mandzhieva S, Bauer T, Kizilkaya R, Zamulina I (2017a) Monitoring of benzo [a] pyrene content in soils under the effect of long-term technogenic pollution. *J Geochem Explor* 174:100–106
- Sushkova SN, Minkina TM, Mandzhieva SS, Deryabkina IG, Vasil'eva GK, Kizilkaya R (2017) Dynamics of benzo[α]pyrene accumulation in soils under the influence of aerotechnogenic emissions. *Eurasian Soil Sci* 50(1):95–105
- Sushkova S, Minkina T, Dudnikova T, Barbashev A, Popov Y, Rajput V, Bauer T, Nazarenko O, Kizilkaya R (2021b) Reduced plant uptake of PAHs from soil amended with sunflower husk biochar. *Eurasian J Soil Sci* 10(4):269–277
- Vannoppen A, Gobin A, Kotova L, Top S, De Cruz L, Viksna A, Aniskevich S, Bobylev L, Buntmeyer L, Caluwaerts S (2020) Wheat yield estimation from NDVI and regional climate models in Latvia. *Remote Sensing* 12:2206
- VROM (1994): Intervention values and target values: soil quality standards; Netherlands Ministry of Housing, Spatial Planning and Environment, Department of Soil Protection, The Hague, Netherlands
- Wilson SC, Jones KC (1993) Bioremediation of soil contaminated with polynuclear aromatic hydrocarbons (PAHs): a review. *Environ Pollut* 81:229–249
- Yu H, Li T, Liu Y, Ma L (2019) Spatial distribution of polycyclic aromatic hydrocarbon contamination in urban soil of China. *Chemosphere* 230:498–509
- Yurdakul S, Çelik I, Çelen M, Öztürk F, Cetin B (2019) Levels, temporal/spatial variations and sources of PAHs and PCBs in soil of a highly industrialized area. *Atmos Pollut Res* 10:1227–1238
- Zhang Y, Huang J, Wang F, Blackburn GA, Zhang HK, Wang X, ... Wei C (2017) An extended PROSPECT: advance in the leaf optical properties model separating total chlorophylls into chlorophyll a and b. *Sci Rep* 7 (1), 1-10
- Zhu L, Chen Z, Wang J, Ding J, Yu Y, Li J, Xiao N, Jiang L, Zheng Y, Rimmington GM (2014) Monitoring plant response to phenanthrene using the red edge of canopy hyperspectral reflectance. *Mar Pollut Bull* 86:332–341

Publisher's note Springer Nature remains neutral with regard to jurisdictional claims in published maps and institutional affiliations.